

CIPS RAA Level 2B Data

Last updated February 2023

1. Introduction

CIPS Rayleigh Albedo Anomaly (RAA) files are provided for levels 2A, 2B, 2C, and 3A. At the current time, the retrieval version is being updated from v1.10r06 to v1.10r07. This document describes the level 2B data product for v1.10r07. Before analyzing level 2B data, users should also read the CIPS instrument overview, data overview, and RAA level 2A documents (see <https://lasp.colorado.edu/aim/documentation>).

Briefly, CIPS RAA Level 2A data files contain CIPS RAA data (RAA, RAA variance, wave properties) in a scene-by-scene format, where a CIPS scene contains simultaneous images from the four CIPS cameras. Users interested in conducting a quantitative analysis of GW properties should use the level 2A data product. The wavelength, amplitude, and phase speed direction of identified waves are provided only in the level 2A data product.

Level 2B data files contain RAA and RAA variance data in an orbit-by-orbit format, merging the level 2A RAA (or RAA variance) data for all scenes in a given orbit via noise-weighted averaging of overlapping pixels from different scenes. There are ~15 orbits per day. Level 2B RAA data and associated geolocation variables are provided with a horizontal resolution of ~56 km² over the entire orbit track (see details of the horizontal resolution in the level 2A documentation).

Users interested in a qualitative view of the wave morphology, but not the wave properties themselves, are encouraged to use the level 2B data product. The advantage of using level 2B is that it provides the context of an entire orbit, and waves are often visible in multiple adjacent scenes. The disadvantage is that, for most of the AIM data set, the scenes overlap one another, so wave properties in the overlap regions can be obscured in the level 2B data. The level 2B data files thus do not contain information about the wave properties.

The level 2C data product is closely related to, and derived directly from, the level 2B data product. However, level 2C is for visualization purposes only, and consists of daily maps (png files) in which the level 2B RAA and RAA variance data for all orbits on a given day are overplotted.

For RAA v01.10r06 and later, two level 2B NetCDF data files for each orbit are provided, along with one png file:

- (1) Geolocation: Includes variables such as date, time, latitude, longitude, solar zenith angle, etc. The file name is *cat.nc ("cat" is short for "catalog").
- (2) Rayleigh Albedo Anomaly (RAA): Includes Rayleigh Albedo, Rayleigh Albedo Anomaly (RAA), RAA uncertainty, FFT-filtered RAA, FFT-filtered RAA variance, and FFT-filtered RAA variance uncertainty. The file name is *alb.nc.
- (3) Plots of RAA and RAA variance for each orbit, along with a global map to show the orbit strip location (one png file per orbit).

Variables contained in the NetCDF files are described in tables at the end of this document. Data arrays in the Level 2B files are reported for all Level 2B pixels, with array dimensions corresponding to the number of elements in the along-track and cross-track directions. For convenience in data handling, the level 2B arrays span the bounding box defined by the entire orbit. However roughly half of these elements correspond to locations where no measurements are made and therefore have fill values. Compressed Level 2B geolocation and albedo NetCDF files are ~22 and 4 MB in size, respectively. Uncompressed file sizes are much larger due to the significant fraction of fill (NaN) values in these files. IDL software tools to read the RAA NetCDF files are available for download from the CU-LASP and NASA SPDF web sites. NetCDF readers for other software packages are available elsewhere (e.g., <http://www.unidata.ucar.edu/software/netcdf/software.html>).

2. Orbit Strip Images

For a quick, qualitative overview of the CIPS data, users are encouraged to peruse the level 2B png files, which contain images of the orbit strips. These images often show visual evidence of GW features that can then be analyzed more carefully using the data in the level 2B and level 2A NetCDF files. Figure 1 shows a few examples of representative level 2B orbit strips.

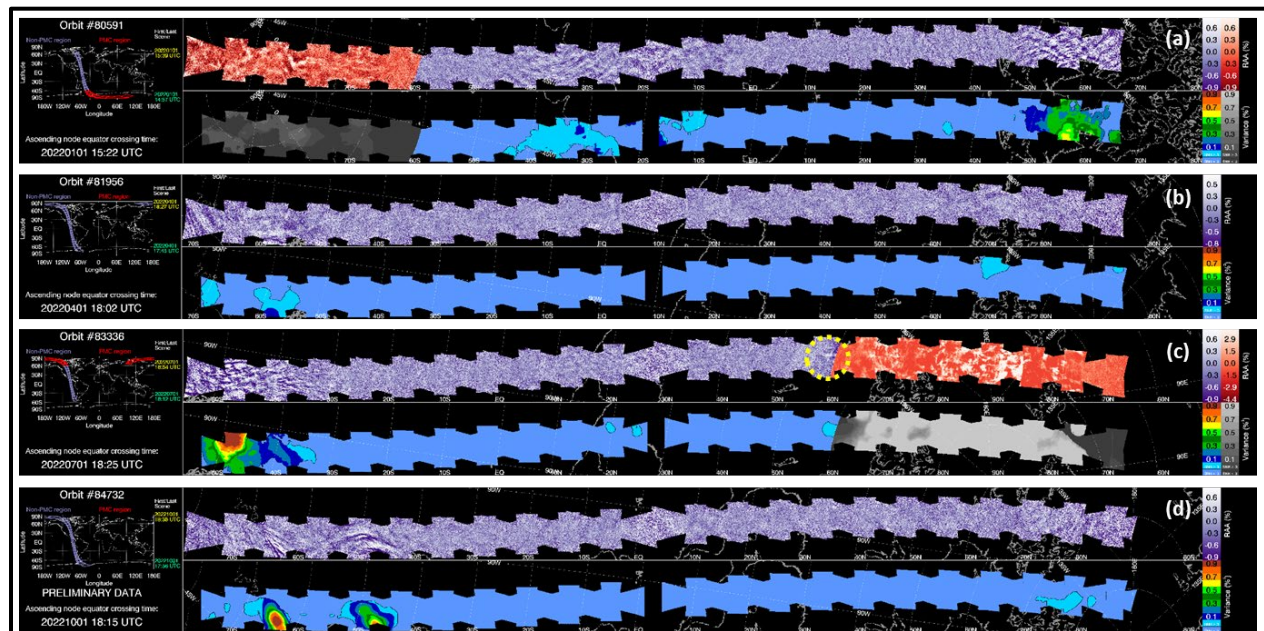


Figure 1. Examples of level 2B orbit strips from (a) 1 January, (b) 1 April, (c) 1 July, and (d) 1 October of 2022. The upper (lower) orbit strip in each panel shows the RAA (RAA variance). The purple (red/orange) color table is used for RAA outside (inside) the nominal PMC region (60° to the pole during PMC seasons). The rainbow (gray) color table is used for the RAA variance outside (inside) the PMC region. The map on the left places the orbit strip into a global context. Signals inside the PMC region are most often due to PMCs near 83 km, not GWs near 53 km.

The level 2A documentation describes some important aspects of these plots, which will not be repeated here. Very briefly, users should be aware of the following:

- Gaps in the middle of the image sequences correspond to the locations of yaw maneuvers and/or calibration images. In Figure 1 the gaps are all caused by yaw maneuvers.

- The RAA variance analysis is only applied to the central part of each scene, which explains why the RAA variance orbit strips do not extend as far on the left edge as the RAA orbit strips in Figure 1.
- PMCs alter the observed albedo, and these effects are not removed from the RAA data products. Therefore, the region where PMCs are most often observed, from 60° to the pole, is shaded red/orange for RAA and gray-scale for RAA variance in the png files during the PMC seasons (~15 May through August in the north and ~15 November through February in the south).
- PMCs can occur at lower latitudes where the png plots are colored in shades of purple, especially during the peak of the PMC season. An example of this is highlighted by the yellow dashed circle in Figure 1c.
- At the time of this writing, data acquired during the period from the 2022 September equinox to the 2023 March equinox are still preliminary, as denoted in the map in Figure 1d (see the File Name Convention notes in section 4 below).

3. Cautions to Users

The level 2A documentation describes the main anomalies or artifacts in the RAA data of which users should be aware. Here we briefly list the issues described in the level 2A documentation, but only describe in detail additional issues that pertain only to the level 2B data product.

Summer Pole Imaging Data. From 2007 until February 2016 CIPS was operating in the summer pole imaging mode. At the time of this writing, RAA data are only available for v1.10r05 (not r06 or r07) for summer pole imaging, and only during the months of March, April, September, and October.

PX Camera Edge Artifacts in v1.10r05 data in 2007-2008. Much of the RAA v1.10r05 data in 2007-2008 exhibit positive RAA artifacts on the edges of the PX camera. The improved calibration in v1.10r07 will likely avoid such artifacts, but this has not yet been demonstrated on a large scale.

Apparent Camera-to-Camera Discontinuities. This issue appears to be associated with images acquired at high SZA or adjacent to a satellite yaw, so users should exercise caution when interpreting regions near these orbit strip edge regions.

Large-Scale Waves. The RAA variance calculation filters out structures in the RAA field with wavelengths longer than 400 km. These structures might therefore appear in a visual inspection of the RAA data, but will not be evident in the RAA variance results. Thus, at the current time, statistical analyses that utilize the RAA variances cannot be used to investigate the occurrence of such large-scale waves.

Signatures of PMCs in the RAA Data. As noted above, signatures of PMCs appear in the RAA data. Users should be cautious when interpreting data at high latitudes in the summer hemisphere, since the observed structure is likely, although not necessarily, caused by PMCs near 83 km altitude, not GWs near 53 km. False structure in the RAA, generally in the form of repeating patterns in adjacent scenes, can also occur at high latitudes in the summer hemisphere, because the principal component analysis used to calibrate the data ignores the PMC region during PMC seasons.

Using RAA Data for PMC Detection. Because PMC signatures are present in the RAA data, and

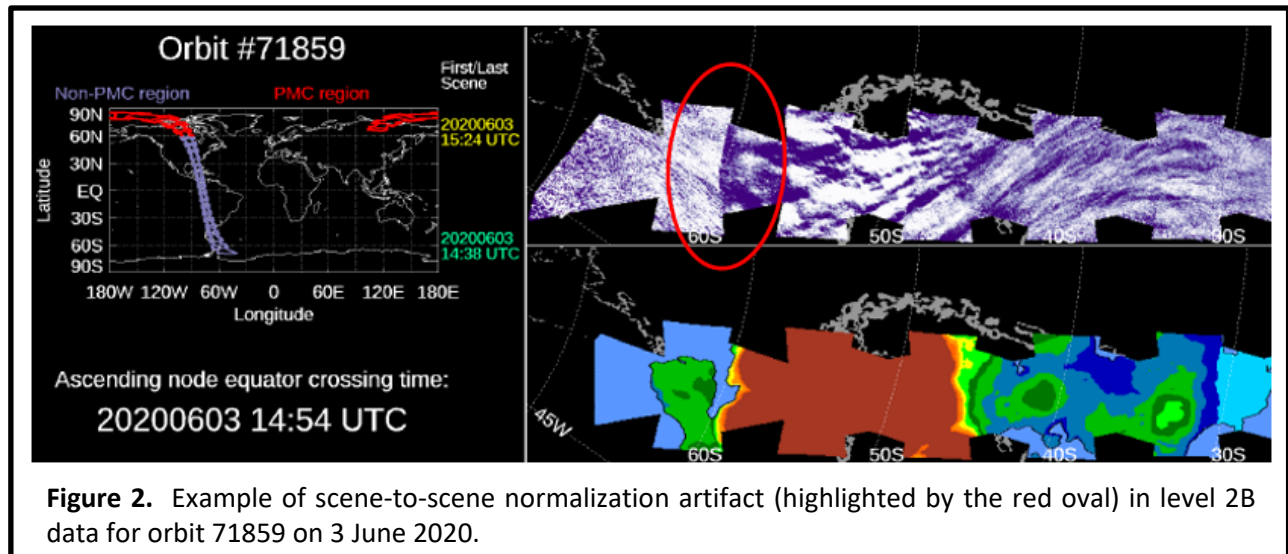
because the RAA retrieval does not impose a false cloud detection threshold, PMCs are often visible in RAA data even though they are not visible in the PMC data. However, since the RAA retrieval is registered to an altitude near 53 km, the RAA data should not be used for quantitative interpretation of PMCs beyond identifying their presence.

PMC vs. RAA Orbit Numbering. Users interested in relating PMC and RAA data should be aware of a change in the AIM orbit-numbering scheme for RAA data beginning on orbit 59351 on 27 February 2018. A major consequence of renumbering the orbits is that the PMC data for all SH seasons beginning with SH1819 will have different orbit numbers than the RAA data. For instance, PMC data in orbit 80596 on 1 Jan 2022 will correspond to SH RAA data in orbit 80597 on 2 Jan 2022.

For more information on all of the cautions noted above, users should see the level 2A documentation. Some issues specific to the level 2B data are described next.

Scene-to-Scene Normalization

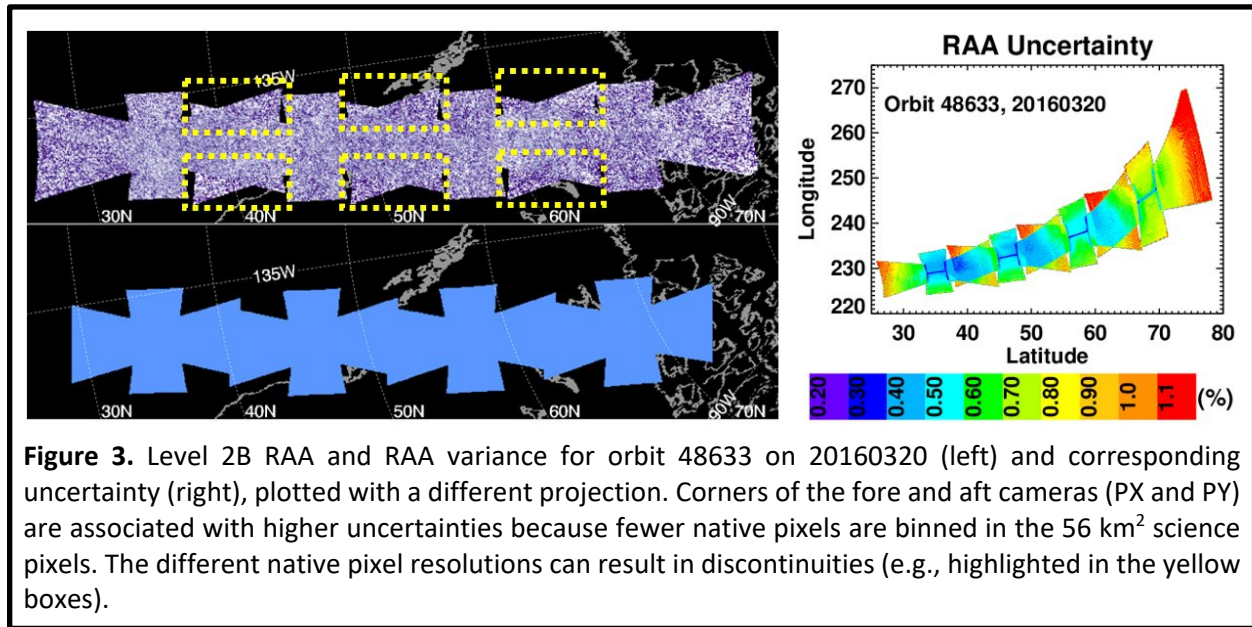
Scene-to-scene normalization can be in error when there is significant large-scale structure that is not fit well by planar gradients similar in size to the camera footprints. This results in discontinuities between scenes, such as depicted in Figure 2 for orbit 71859 on 3 June 2020. Correcting for this error is impractical at the current time, since it would require significant changes to the retrievals. However, the error by definition does not affect level 2A, so wave characteristics in the level 2A data are robust, even if scene-to-scene normalization in level 2B is not correct.



Discontinuities at Camera Corner Overlap Regions

Users will note that in some level 2B data, subtle discontinuities appear in regions where the edge of one camera overlaps with a corner of the fore or aft camera. An example of this is shown in Figure 3, for orbit 48633 on 20 March 2016. These discontinuities reflect the fact that camera pixels in the fore and aft corner regions are elongated relative to other pixels. The science data is binned into "science pixels" that all have a uniform area of 56.25 km², so this means that more native pixels (4 km²) are combined into each science pixel in the nadir than in the fore and aft regions of the scenes. The result is that there is often larger uncertainty in the fore and aft regions than in the

nadir or near-nadir regions. Figure 3 shows part of the level 2B png image for orbit 48633, with the discontinuity regions highlighted by the yellow boxes. Figure 3 also shows the RAA uncertainty for this portion of the orbit. The uncertainty is plotted with a different projection than the RAA itself, but clearly shows the higher uncertainty in the corners of the fore and aft cameras. The discontinuities in the level 2B png images occur at the boundary between regions where pixels in one camera are closer to nadir than the pixels in the overlapping camera. The pixels closer to nadir have lower uncertainties, whereas the fore or aft pixels have higher uncertainties. As with all data sets, users should consider the uncertainties when analyzing the CIPS data.



4. NetCDF Files

The NetCDF files listed in Section 1 enable users to quantitatively analyze the level 2B RAA data plotted in the orbit strip images. The tables below summarize the contents of each data file and provide a brief description of all parameters and arrays. For more information on variables associated with the SZA corrections, orbit track grid, and principal component analysis, users should consult the level 2A documentation.

File name convention: Each file has a day-of-year included in the file name. This is the UT day corresponding to the ascending node equator crossing time, which is the official orbit start time. When the equator crossing time is shortly prior to midnight UT, some or all of the data in the file might have been acquired on the day after the day in the filename. Also, as explained in the level 2A documentation, when the ascending node equator crossing time is on the sunlit side of the orbit, some of the data in the file might have been acquired prior to this time. In addition, file names can include a "preliminary" tag, which indicates that the data have not yet been processed with both the final satellite ephemeris and final instrument calibration data. Preliminary RAA data products are typically released to the public within ~2 days of acquisition. Definitive data with final satellite ephemeris and instrument calibration data are released in 6-month increments, between the March and September equinoxes. At the time of this writing, data acquired during the period from

the 2022 September equinox to the 2023 March equinox are still preliminary, as denoted in the map in Figure 1d above.

Table 1. Variables in the CIPS RAA Level 2B geolocation file. Fill value is NaN.

Variable Name	Units	Type/Dimension	Description
AIM_ORBIT_NUMBER	N/A	Long / 1	NASA orbit number ^(a)
BBOX	pixels	Long / [4]	Bounding Box: Bottom-left indices (x0, y0) and size of box (xsize, ysize) within the larger orbit track grid [x0, y0, xsize, ysize]
CENTER_LON	degrees	Double / 1	Center longitude of orbit at maximum orbit track latitude (~82.5°) in the spring/summer hemisphere; divides ascending and descending node.
DATA_PRODUCT	N/A	String ^(b) / 1	Brief description of the data product
HIGH_SZA_SYSTEMATIC_CORRECTION_NORTH	%	Float / [201]	PCA-based, SZA-dependent correction added to northern hemisphere RAA with SZA>75°
HIGH_SZA_SYSTEMATIC_CORRECTION_SOUTH	%	Float / [201]	PCA-based, SZA-dependent correction added to southern hemisphere RAA with SZA>75°
HIGH_SZA_SYSTEMATIC_CORRECTION_SZA_GRID	degrees	Float / [201]	SZA grid for high SZA corrections; interpolate off this grid to recover corrections at other SZAs
KM_PER_PIXEL	km	Float / 1	Linear dimension of square pixel occupying area of CIPS resolution element
LATITUDE	degrees	Float / [Xdim,Ydim]	Latitude of each element
LONGITUDE	degrees	Float / [Xdim,Ydim]	Longitude of each element; ranges from -180 to 180
NLAYERS	N/A	Integer / [Xdim,Ydim]	Number of scenes from which level 2A pixels were merged, for each 2B pixel
NOTES	N/A	String ^(b) / 1	Any additional notes
ORBIT_END_TIME	micro-seconds	Double / 1	GPS end time of AIM_ORBIT_NUMBER (microseconds from 0000 UT on 6 Jan 1980)
ORBIT_START_TIME	micro-seconds	Double / 1	GPS start time of AIM_ORBIT_NUMBER (microseconds from 0000 UT on 6 Jan 1980)
ORBIT_START_TIME_UT	N/A	String ^(b) / 1	String for UT start time of orbit
ORBIT_TRACK_EPOCH	micro-seconds	Double / 1	GPS time at which the orbit track axis approximately matches the true orbit track. ^(c)
ORBIT_TRACK_X_AXIS	N/A	Double / [3]	X axis on which the orbit track grid is defined, for levels 2A and 2B, in Earth-centered, Earth-fixed (ECEF) coordinates
ORBIT_TRACK_Y_AXIS	N/A	Double / [3]	Y axis on which the orbit track grid is defined, for levels 2A and 2B, in ECEF coordinates
ORBIT_TRACK_Z_AXIS	N/A	Double / [3]	Z axis on which the orbit track grid is defined, for levels 2A and 2B, in ECEF coordinates
PCA_ORBIT_RANGE	N/A	Long / [2]	Orbit range over which the PCA was run
PRODUCT_CREATION_TIME	N/A	String ^(b) / 1	String containing UT time at which data file was produced
REVISION	N/A	String ^(b) / 1	Data revision number
UT_DATE	yyyymmdd	Long / [Xdim,Ydim]	UT date for each pixel; average of all scenes that included the geographic grid cell for the pixel

UT_DATE_ORBIT_START	yyyymm dd	String ^(b) / 1	UT date of AIM_ORBIT_NUMBER start time (ascending node equator crossing time); CIPS file names use this date
UT_TIME	hour of day	Float / [Xdim,Ydim]	UT time for each pixel; average of all scenes that included the geographic grid cell for the pixel
VERSION	N/A	String ^(b) / 1	Data version number
XDIM	N/A	Long / 1	Number of along-orbit-track elements (pixels) in the data arrays
YDIM	N/A	Long / 1	Number of cross-orbit-track elements (pixels) in the data arrays
ZENITH_ANGLE	degrees	Double / [Xdim,Ydim]	Solar zenith angle (SZA) of each element, referenced to 50 km altitude

^(a) After Sept 2017, orbits are spliced with second half of AIM_ORBIT_NUMBER-1 to produce continuous dayside data, in which case this is the orbit number for the northern half of the data.

^(b) Depending on the read software, these variables might appear as Byte rather than string. If so, they should be converted to string.

^(c) Due to the rotation of the earth the orbit track doesn't trace out a plane in earth-fixed coordinates.

Table 2. Variables in the CIPS RAA Level 2B Rayleigh Albedo Anomaly file. Fill value is NaN.

Variable Name	Units	Type/Dimension	Description
FILTERED_RAA	%	Float / [Xdim,Ydim]	Spatial domain inversion of the spectrally filtered RAA for each pixel; noise-weighted average of level 2A pixels from scenes that include the geographic grid cell for the pixel
FILTERED_RAA_VARIANCE	% ²	Float / [Xdim,Ydim]	Variance of spectrally filtered RAA; calculated from filtered RAA to ensure continuity across scenes
FILTERED_RAA_VARIANCE_UNC	% ²	Float / [Xdim,Ydim]	Uncertainty in variance of spectrally filtered RAA; additional smoothing applied to smooth transition between scenes
RAYLEIGH_ALBEDO	10 ⁻⁶ sr ⁻¹	Float / [Xdim,Ydim]	Total observed albedo for each pixel; noise-weighted average of level 2A pixels from scenes that include the geographic grid cell for the pixel
RAYLEIGH_ALBEDO_ANOMALY	%	Float / [Xdim,Ydim]	100*(observed_albedo-baseline)/baseline, where baseline = basic_state_albedo; noise-weighted average of level 2A pixels from scenes that include the geographic grid cell for the pixel
RAYLEIGH_ALBEDO_ANOMALY_UNC	%	Float / [Xdim,Ydim]	Uncertainty in RAA due to noise. Propagation of noise error due to the weighted average that is applied to the level 2A RAA.

5. References

Bailey, S. M., G. E. Thomas, D. W. Rusch, A. W. Merkel, C. D. Jeppesen, J. N. Carstens, C. E. Randall, W. W. McClintock, and J. M. Russell III (2009), Phase functions of polar mesospheric cloud ice as observed by the CIPS instrument on the AIM satellite, *J. Atmos. Sol. Terr. Phys.*, **71**, 373–380, doi:10.1016/j.jastp.2008.09.039.

Lumpe, J. D., S.M. Bailey, J.N. Carstens, C.E. Randall, D. Rusch, G.E. Thomas, K. Nielsen, C. Jeppesen,

W.E. McClintock, A.W. Merkel, L. Riesberg, B. Templeman, G. Baumgarten, and J.M. Russell, III (2013), Retrieval of polar mesospheric cloud properties from CIPS: algorithm description, error analysis and cloud detection sensitivity, *J. Atmos. Solar-Terr. Phys.*, <http://dx.doi.org/10.1016/j.jastp.2013.06.007>.

McPeters, R. D. (1980), The behavior of ozone near the stratopause from two years of BUW observation, *J. Geophys. Res.*, 85, 4545–4550, doi:10.1029/JC085iC08p04545.

Randall, C. E., J. Carstens, J. A. France, V. L. Harvey, L. Hoffmann, S. M. Bailey, M. J. Alexander, J. D. Lumpe, J. Yue, B. Thuraijah, D. E. Siskind, Y. Zhao, M. J. Taylor, and J. M. Russell, III (2017), New AIM/CIPS global observations of gravity waves near 50-55 km, *Geophys. Res. Lett.*, 44, 7044–7052, <http://dx.doi.org/10.1002/2017GL073943>.

Created by Jerry Lumpe and Cora Randall, June 2017.